Local Gaussian process extrapolation for BART models with applications to causal inference

Meijia Wang*, Jingyu He[†] and P. Richard Hahn*

Abstract. Bayesian additive regression trees (BART) is a semi-parametric regression model offering state-of-the-art performance on out-of-sample prediction. Despite this success, standard implementations of BART typically provide inaccurate prediction and overly narrow prediction intervals at points outside the range of the training data. This paper proposes a novel extrapolation strategy that grafts Gaussian processes to the leaf nodes in BART for predicting points outside the range of the observed data. The new method is compared to standard BART implementations and recent frequentist resampling-based methods for predictive inference. We apply the new approach to a challenging problem from causal inference, wherein for some regions of predictor space, only treated or untreated units are observed (but not both). In simulations studies, the new approach boasts superior performance compared to popular alternatives, such as Jackknife+.

Keywords: Tree, Extrapolation, Gaussian process, Predictive interval, XBART, XBCF.

1 Introduction

Tree-based supervised learning algorithms, such as the Classification and Regression Tree (CART) (Breiman et al., 1984), Random Forests (Breiman, 2001), and XGBoost (Chen and Guestrin, 2016) are popular in practice due to their ability to learn complex nonlinear functions efficiently. Bayesian Additive Regression Trees (BART, Chipman et al. (2010)) is the most popular model-based regression tree method; it has been demonstrated empirically to provide accurate out-of-sample prediction and its Bayesian uncertainty intervals often out-perform alternatives in terms of frequentist coverage. XBART (He and Hahn, 2021) is a stochastic tree ensemble method that can be used to approximate BART models in a fraction of the run-time. Throughout the paper we will refer to BART models, but will use the XBART fitting algorithm.

While tree-based methods frequently provide accurate out-of-sample predictions, their ability to extrapolate is fundamentally limited by their intrinsic structure, which is piecewise constant. Trees partition the covariate space into disjoint rectangular regions (leaf nodes) based on the observed covariates, then estimate a simple model (typically a constant) based on training data falling in the corresponding region. Consequently, to predict testing data outside the observed range of covariates in the training, a naive tree regression model would extrapolate the constant in whatever leaf node that point falls in. Figure 1 illustrates the potential problem of extrapolation for the traditional tree models with constant leaf parameters in one-dimensional covariate space. If the

^{*}Arizona State University mwang164@asu.edu prhahn@asu.edu

[†]City University of Hong Kong jingyuhe@cityu.edu.hk

testing data lie out of the range of the training, tree models have to extrapolate using the constant leaf parameter in the corresponding leaf node regardless of how far away the testing observations are from the nearest training point.

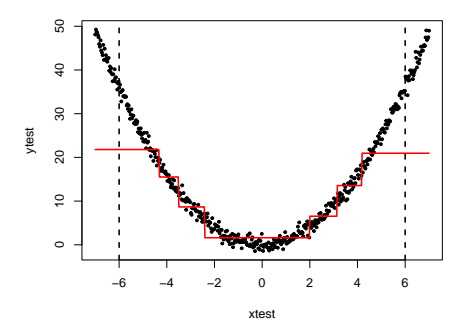


Figure 1: An example of the traditional tree extrapolation. The synthetic training data are black points. The fitted CART model is the step function in the red line. The two vertical dashed lines are testing data to predict, which are outside the range of the training data. The traditional tree algorithms with constant leaf parameters extrapolate the prediction by a constant of the corresponding leaf node.

In addition to poor point predictions, a flawed extrapolation model likewise impairs posterior prediction intervals. Ideally, a BART model would predict essentially according to the prior at points far from the observed data; standard implementations instead never sample cutpoints beyond the training range and consequently dramatically understate the uncertainty in the unknown function in extrapolation regions. As a result, the coverage of predictive intervals from standard tree-based methods can be poor. While regression tree methods can be used in conjunction with resampling approaches to construct improved prediction intervals (Efron and Stein, 1981; Papadopoulos, 2008; Vovk, 2015; Barber et al., 2021), such a strategy does not solve the intrinsically poor extrapolation of regression trees.

This paper presents a novel approach to help tree methods extrapolate the exterior points and construct prediction intervals. The new method (XBART-GP) fits a Gaussian process (GP) at each leaf node of a BART tree and predicts exterior test points in the leaf by the associated GP model. Our approach differs from a treed Gaussian process (Gramacy and Lee, 2008) in that the local GP extrapolation does not impact the initial BART model fit. Loosely speaking, the model of Gramacy and Lee (2008) is a "treed" GP while our approach is "GPed" tree. The local GP extrapolation defines a novel posterior predictive distribution in terms of BART posterior samples and a GP model; it is not a new likelihood for inferring the trees themselves. Rather, the BART-inferred trees are used as inputs to the novel posterior predictive specification (cf. section 3).

We compare our approach with recently proposed alternatives such as Jackknife+ (Barber et al., 2021) in simulation studies. Our results illustrate that XBART-GP

achieves nearly the desired coverage on out-of-range data while not substantially inflating the interval length.

Additionally, our new extrapolation method is illustrated with an application to causal inference. When only treated (untreated) units are observable in a particular region of covariate space, inferring the untreated (treated) potential outcomes requires extrapolating the untreated (treat) response surface into that region. Such a scenario is said to violate the positivity condition necessary for identifying causal effects from observational data. Previous work on positivity violation include (D'Amour et al., 2021), who focus on high-dimensional covariate spaces; (Nethery et al., 2019), who propose a spline model to extrapolate in non-overlap regions; and (Zhu et al., 2022), who construct a Gaussian process for the entire covariate space. In this paper, we apply the proposed local GP extrapolation approach to the Bayesian causal forest model (Hahn et al., 2020; Krantsevich et al., 2022).

The rest of the paper is organized as follows. Section 2 reviews Gaussian processes, BART, Jackknife+, and Bayesian causal forests. Section 3 develops the new approach in detail and presents simulation studies demonstrating its advantages over the current state-of-the-art. Section 4 adapts the method to the causal inference context and presents simulation results showing that local GP extrapolation of BART models can handle substantial violations of the overlap condition.

2 Background

2.1 Notation

We clarify notations throughout the paper. Let $\mathbf{x} = (x^{(1)}, \dots, x^{(p)})$ denote a *p*-dimensional covariate vector, or regressors. Capital letter $\mathbf{X} = (\mathbf{x}'_1, \dots, \mathbf{x}'_n)'$ denotes the $n \times p$ predictor matrix, and $\mathbf{y} = (y_1, \dots, y_n)$ is a vector of target values for supervised learning. First, we demonstrate our approach under the standard regression setting,

$$y_i = f(\mathbf{x}_i) + \epsilon_i, \quad \epsilon_i \sim N(0, \sigma^2),$$
 (2.1)

where we assume the residual term ϵ is a Gaussian noise term with mean zero and variance σ^2 .

Let $C_{n,\alpha}(\mathbf{x})$ denote the prediction interval for a test point \mathbf{x} with confidence level $1-\alpha$ given n predicted values. Notations $q_{n,\alpha/2}^-\{y_i\}$ and $q_{n,\alpha/2}^+\{y_i\}$ are the quantile functions for the $\lceil (1-\alpha/2)(n+1) \rceil$ -th smallet value and the $\lfloor \alpha/2(n+1) \rfloor$ -th smallest value among a set of values $\{y_1,\ldots,y_n\}$ respectively.

2.2 BART model and XBART algorithm

The BART model (Chipman et al., 2010) assumes that the unknown function f(x) in the regression model (2.1) can be approximated by a sum of regression trees, i.e.

$$f(\mathbf{x}) = \sum_{l=1}^{L} g(\mathbf{x}, \mathbf{T}_l, \mu_l),$$
 (2.2)

where T_l represents a tree structure, which is a set of split rules partitioning the covariate space, and μ_l is a vector of leaf parameters associated with the leaf nodes in tree T_l .

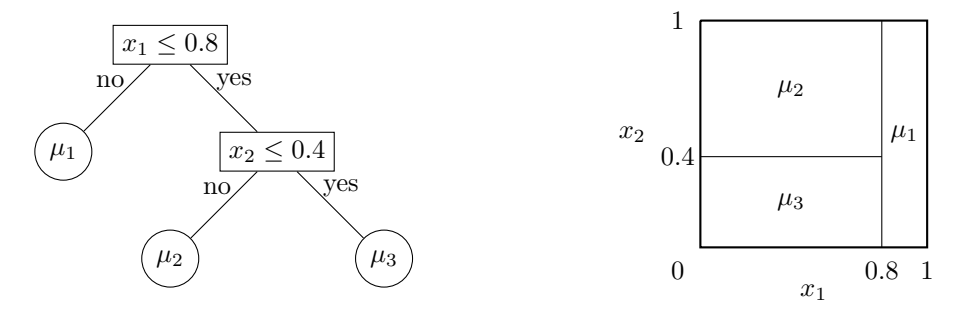


Figure 2: A regression tree partitions a two-dimensional covariate space (right) with two internal decision nodes (left). Each element of the partition corresponds to a terminal node in the tree with leaf parameter μ_l .

Figure 2 illustrates a binary regression tree. The tree consists of a set of internal decision nodes that partition the covariate space to a set of terminal nodes (leaf nodes, say $\{A_1, \dots, A_B\}$). The tree function $g(\mathbf{x}, \mathbf{T}_l, \mu_l)$ is essentially a step function due to the constant leaf parameter. It assigns point \mathbf{x} with the leaf parameter of the leaf node that it falls into in tree \mathbf{T}_l .

Trees are known to be prone to overfitting due to its high flexibility. Thus, proper regularization is necessary to achieve good out-of-the-sample performance. BART assigns a regularization prior to the tree structure that strongly favors weak, or small trees. The tree prior $p(T_l)$ specifies the probability for a node to split into two child nodes at depth d to be

$$\alpha(1+d)^{-\beta}, \quad \alpha \in (0,1), \, \beta \in [0,\infty), \tag{2.3}$$

which decreases exponentially as tree grows deeper, implying strong regularization on the size of the tree. Chipman et al. (2010) suggest choosing $\alpha = 0.95$ and $\beta = 2$. The prior of each leaf parameter $p(\mu_{lb})$ is assumed to be independent normal with variance τ , i.e. $\mu_{lb} \sim N(0, \tau)$. The prior of the residual variance σ^2 is set to be inverse-Gamma(a, b).

The ensemble of trees is fitted by Bayesian backfitting and MCMC sampling scheme. Let T_{-l} denotes the set of all trees except T_l , and similarly define μ_{-l} . Note that the conditional posterior $p(T_l, \mu_l \mid T_{-l}, \mu_{-l}, \sigma^2, y)$ depends on other trees and parameters only through the residuals

$$\mathbf{r}_l := y - \sum_{h \neq l} g(\mathbf{x}, \widehat{\mathbf{T}}_h, \widehat{\mu}_h) = g(\mathbf{x}, \mathbf{T}_l, \mu_l). \tag{2.4}$$

Furthermore, one can integrate out the conjugate prior of μ_l and derive the posterior of a tree T_l in closed form, i.e.

$$p(\mathbf{T}_l \mid \mathbf{r}_l, \sigma^2) \propto p(\mathbf{T}_l) \int p(\mathbf{r}_l \mid \mu_l, \mathbf{T}_l, \sigma^2) p(\mu_l \mid \mathbf{T}_l, \sigma^2) d\mu_l.$$
 (2.5)

This allows the conditional posterior $T_l \mid r_l, \sigma^2$ and $\mu_l \mid T_l, r_l, \sigma^2$ to be drawn separately and sequentially for l = 1, ..., L. After all trees are grown (we call it a sweep), the residual variance σ^2 is then sampled from the full conditional $\sigma^2 \mid T_1, \dots, T_L, \mu_1, \dots, \mu_L, y$.

The original BART model (Chipman et al., 2010) draws trees from the posterior using a random walk Metropolis-Hastings (MH-MCMC) algorithm. Per iteration, the algorithm randomly proposes a single growing or pruning procedure to each tree and accept or reject according to the MH ratios. Since the proposal in each iteration only makes small modification, one can expect it is not efficient for the MH-MCMC algorithm to explore the posterior model space. The experiments in (Chipman et al., 2010) typically use 200 burn-in steps and 1000 iterations with 200 trees. Furthermore, the algorithm does not scale well with large size of data observations or covariates. XBART (He et al., 2019; He and Hahn, 2021), shortened for accelerated Bayesian additive regression trees, is a stochastic tree ensemble method inspired by BART. The essential idea of XBART is to avoid the expensive MH-MCMC computation but grow complete new trees recursively (like CART) using the marginal likelihood and regularization implied by BART as the split criterion. Therefore it is much more efficient to explore the posterior of BART, and scales well. Our approach is designed for both the framework of XBART and BART, while we will demonstrate the performance using XBART for the reason of computational efficiency.

Next we review XBART algorithm. Consider a dataset with P variables and we pick C cutpoints for each variable. At each node, the algorithm considers $C \times P$ cutpoints in addition to a null cutpoint corresponding stop splitting the current node (no-split option). Each of the cutpoint (p,c) splits the node along variable x_p at value c and partition the data into two subsets. Let $s(\leq, p, c)$ and $s(\geq, p, c)$ denote the sufficient statistics that summarize the two subsets. Furthermore, XBART allows the tree growing process terminating early, the sufficient statistics for the null cutpoint (stop splitting the current node) is $s(\emptyset)$. Let $l(s(\cdot))$ denote the marginal log-likelihood of the data that falls into a child node with sufficent statistics $s(\cdot)$. The probability of choosing a splitrule (p,c) is proportional to its marginal likelihood over the marginal likelihood of all available split-rules, i.e.,

$$\pi(p,c) = \frac{\exp(l(s(\leq, p, c)) + l(s(\geq, p, c)))}{\sum_{p=1}^{P} \sum_{c=1}^{C} \exp(l(s(\leq, p, c)) + l(s(\geq, p, c))) + \exp(l(s(\emptyset)))\kappa(d)},$$
 (2.6)

where $\kappa(d) = \frac{1-\alpha(1+d)^{-\beta}}{\alpha(1+d)^{-\beta}}$ is the weight for the option of stop splitting the current node.

By this construction, the prior probability of splitting the current node (regardless of which split point) is $\alpha(1+d)^{-\beta}$, which is in line with the tree prior in BART (2.3) to inherit its regularization performance. The forests of XBART grow similarly as BART using Bayesian backfitting. Each tree fits residuals of all other trees as defined in equation 2.4. XBART differs from BART by updating the forest multiple times. Once all trees in the forest are updated (finish one sweep), XBART starts over to update all trees again to sample the next sweep. The algorithm terminates until drawing a pre-specified number of sweeps.

To obtain posterior prediction interval from XBART, we take the sampled trees as draws from a standard Bayesian Monte Carlo algorithm. Suppose the algorithm draws S

sweeps with S_0 burn-out iterations and L trees per forest. The predicted posterior mean and variance at iteration s are defined as $\hat{f}_s(\mathbf{x}) = \sum_{l=1}^L g_l(\mathbf{x}, \widehat{\mathbf{T}}_l^{(s)}, \widehat{\mu}_l^{(s)})$ and $\widehat{\sigma}_s^2$ respectively. The final prediction of target value \widehat{y}_s is sampled from $N(\widehat{f}_s(\mathbf{x}), \widehat{\sigma}_s^2)$. Furthermore, the prediction interval of target level $1 - \alpha$ is given by quantiles of the predictions as follows

$$\widehat{C}_{S,\alpha}^{\mathrm{XBART}}(\mathbf{x}) = \left[\widehat{q}_{S,\alpha/2}^{-}\{\widehat{y}_s\}, \widehat{q}_{S,\alpha/2}^{+}\{\widehat{y}_s\}\right]. \tag{2.7}$$

Note that this definition of posterior prediction interval is based on the prediction of every single tree with a constant leaf parameter, i.e., it still suffers from the extrapolation problem when the testing data is out of the range of the training.

2.3 Gaussian process regression

This section reviews Gaussian process regression, a critical ingredient of the proposed XBART-GP extrapolation. Gaussian process regression is a non-parametric kernel-based Bayesian probabilistic model. It has the ability to interpolate and extrapolate as the covariance defines the model's behavior over its full domain. Essentially, the specified covariance function characterizes the linear dependence of the response at pairs of points as a function of some measure of distance between those points in covariate space. For a textbook treatment of the Gaussian process, see Rasmussen (2003).

More specifically, a Gaussian process model assumes that $\{f(\mathbf{x}), \mathbf{x} \in \mathbb{R}^p\}$ is a set of random variables that follows Gaussian process with some mean function $\mu(\mathbf{x})$ and covariance function $k(\mathbf{x}, \mathbf{x}')$. The GP model assumes that given a new data point \mathbf{x}' and a matirx of training data $\mathbf{X} = (\mathbf{x}_1, \dots, \mathbf{x}_n)'$ of size $n \times p$, the joint distribution of the corresponding truth means $\{f(\mathbf{x}'), f(\mathbf{x}_1), \dots, f(\mathbf{x}_n)\}$ follows a multivariate Gaussian distribution. Since in most regression problems, we can only observe the values y instead of the true functions. The joint distribution of a test point $f(\mathbf{x}')$ and the observed values y is

$$\begin{pmatrix} f(\mathbf{x}') \\ \mathbf{y} \end{pmatrix} \sim N \left(\mu \begin{pmatrix} \mathbf{x}' \\ \mathbf{X} \end{pmatrix}, \begin{pmatrix} \sigma_{\mathbf{x}'}, & \Sigma_{\mathbf{x}'\mathbf{X}} \\ \Sigma_{\mathbf{X}\mathbf{x}'}, & \Sigma_{\mathbf{X}\mathbf{X}} + \sigma_{\mathbf{x}'}^2 \mathbf{I} \end{pmatrix} \right)$$
(2.8)

where $\mu(\cdot)$ is a regression function and the covariance matrices are calculated by covariance function $k(\mathbf{x}, \mathbf{x}')$ with the user's choice. The covariance terms are $\sigma_{\mathbf{x}'}^2 = k(\mathbf{x}', \mathbf{x}')$, $\Sigma_{\mathbf{x}'\mathbf{X}} = \Sigma_{\mathbf{X}\mathbf{x}'}^T = k(\mathbf{x}', \mathbf{X})$, and $\Sigma_{\mathbf{X}\mathbf{X}} = k(\mathbf{X}, \mathbf{X})$ defined by the covariance function.

The prediction of the outcome $f(\mathbf{x}')$ can be drawn from the Gaussian distributions, conditional on covariates \mathbf{x}' , $\mathbf{X} = \{\mathbf{x}_1, \dots, \mathbf{x}_n\}$ and observed values \mathbf{y} , or $f(\mathbf{x}') \sim N(\mu_{\mathbf{x}'|\mathbf{X}}, \sigma_{\mathbf{x}'|\mathbf{X}})$ with conditional mean and covariance as follows:

$$\mu_{\mathbf{x}'|\mathbf{X}} = \mu(\mathbf{x}') + \Sigma_{\mathbf{x}'\mathbf{X}} \left[\Sigma_{\mathbf{X}\mathbf{X}} + \sigma^2 \mathbf{I} \right]^{-1} (\mathbf{y} - \mu(\mathbf{X}))$$
 (2.9)

$$\Sigma_{\mathbf{x}'|\mathbf{X}} = k(\mathbf{x}', \mathbf{x}') - \Sigma_{\mathbf{x}'\mathbf{X}} \left[\Sigma_{\mathbf{X}\mathbf{X}} + \sigma^2 \mathbf{I} \right]^{-1} \Sigma_{\mathbf{X}\mathbf{x}'}.$$
 (2.10)

It is straightforward to draw samples from the Gaussian conditional distribution, and the predictive interval is defined by quantiles of the samples with the given confidence level.

2.4 Predictive confidence interval by Jackknife+

We will compare the new method to alternative approaches on the basis of frequentist coverage. Several of those alternative methods are explicitly designed with frequentist coverage in mind. Here we briefly review the previous literature on such approaches.

Well known frequentist approaches to constructing prediction intervals include the Jackknife (Efron and Stein, 1981), inductive conformal prediction (Papadopoulos, 2008), and cross-conformal prediction (Vovk, 2015). Recently, the Jackknife+ method (Barber et al., 2021) has emerged as the state-of-the-art method for constructing predictive confidence intervals. Whereas the standard Jackknife creates confidence intervals using quantiles of leave-one-out residuals, Jackknife+ takes a similar approach, using the leave-one-out predictions at the test point to account for the uncertainty in the prediction. In this paper, we mainly compare the predictive confidence interval of our GP extrapolation with that of the latest Jackknife+ method and its cross-validation version. For a brief introduction to Jackknife+, see the Appendix.

Jackknife+ and CV+ share similar advantages, such as the coverage is guaranteed to be bounded by some constant equals or closed to the target level $1 - \alpha$. However, this property does not extend to the case where the training and testing data are not exchangeable. Neither of them can extrapolate *exterior* points and provide predictive interval with nominal coverage.

2.5 Overlap and extrapolation in treatment effect estimation

A motivating example of an applied extrapolation problem occurs in treatment effect estimation, in particular, when one of the necessary assumption is violated under the potential outcome framework (Imbens and Rubin, 2015) for estimating the treatment effect

Let Y denote the response variable and Z denote the binary treatment variable. The treatment effect on an individual x_i , denoted as $\tau(x_i)$, is the difference between the response values when the treatment is set to $Z_i = 1$ versus $Z_i = 0$. Since one can not observe both outcomes at the same time, the potential outcome framework formalizes this problem by using $Y_i(1)$ and $Y_i(0)$ to denote the potential outcome under treatment and control for a unit. The observable outcome can be expressed as $Y_i = Z_i Y_i(1) + (1 - Z_i) Y_i(0)$.

Most causal inference methods using the potential outcome framework also rely on the following assumptions: 1) Stable Unit Treatment Value Assumption (SUTVA); 2) Strong ignorability assumption. The second assumption states that there are no unmeasured confounders, i.e., $Y_i(1), Y_i(0) \perp \!\!\! \perp Z_i \mid \mathbf{X}_i$, and every individual has a positive probability of being treated: $0 < P(Z_i = 1 \mid \mathbf{x}_i) < 1$. However, the latter does not hold in many cases; even if it holds in principle, with small sample sizes and high dimensional control variables, effective violations of overlap are common (D'Amour et al., 2021).

"Solving" the problem of poor overlap can be handled in one of two ways. One can "trim" the population (Ho et al., 2007; Petersen et al., 2012; Crump et al., 2009),

thereby estimating the treatment effect restricted to the overlap region. This approach is inappropriate when the average treatment effect over the entire population is required (Yang and Ding, 2018) or when conditional average treatment effects are of interest. In these cases, the second strategy is to perform model-based extrapolation, extending an estimated response surface into regions where no data was observed. Variations of this strategy have been the focus of recent research. Li et al. (2018a) and Li et al. (2018b) proposed using overlap weights to balance the covariates for estimating the average treatment effect. Zhu et al. (2022) propose a Gaussian process model for extrapolation necessitated by overlap violations.

Most similar to the present work is Nethery et al. (2019), who propose a data-driven definition of overlap and non-overlap regions, and use BART for prediction in the overlap area and a spline model for extrapolating the trend in the non-overlap area. Our work differs from Nethery et al. (2019) in that we use the BART fit itself to define the overlap region as well as to define the covariance function in our GP extrapolation model. Moreover, we directly extrapolate the treatment effect surface as learned by a Bayesian causal forest (BCF) model (Hahn et al., 2020; Krantsevich et al., 2022). The BCF model is a combination of two BART models, with the following representation

$$f(\mathbf{x}_i, z_i) = \mu(\mathbf{x}_i) + \tau(\mathbf{x}_i)z_i \tag{2.11}$$

where μ and τ are the referred to as the prognostic and treatment effect functions, respectively. This representation allows us to extrapolate $\tau(x)$ directly, whereas Nethery et al. (2019) extrapolate the treated and untreated response surfaces individually.

3 Local GP extrapolation for BART

Traditional BART prediction intervals in Equation (2.7) provide good coverage with tight intervals on many data generating processes (He and Hahn, 2021) with exchangeable train and test data. However, when the train and test sets differ substantially in terms of their support, predictions are less reliable. The intuition behind our method is to use the tried-and-true BART predictions (and intervals) for prediction points within the range of the training data, but to incorporate Gaussian process extrapolation for points well outside this support. Therefore, the first step in describing the new method is to formally define the concepts of exterior points in the context of regression trees. In specific, we will define extrapolation points locally in terms of the regression trees: a test point \mathbf{x}' is an exterior point if and only if it is outside the range of the training data in the leaf node it falls in. The basic strategy of the new method is to use the leaf-specific training data to extrapolate such exterior points using a local Gaussian process. Combining these local GP predictions across trees (and across posterior samples) constitutes the main technical content of the new method, details of which are below.

Before getting into those details, a big-picture explanation may be helpful. Typically, a Bayesian posterior predictive distribution is expressed as:

$$f(\tilde{y} \mid y_{1:n}, \mathbf{X}_{1:n}) = \int f(\tilde{y} \mid \theta) \pi(\theta \mid y_{1:n}, \mathbf{X}_{1:n}) d\theta,$$

which conveys the idea that future and past data are conditionally independent given the model parameters. Here, we explicitly deviate from this formulation, but only for those future points that are exterior (defined as a function of the model parameters). For such a point, our posterior predictive is defined as

$$f(\tilde{y} \mid y_{1:n}, \mathbf{X}_{1:n}) = \int f(\tilde{y} \mid \theta, y_{1:n}, \mathbf{X}_{1:n}) \pi(\theta \mid y_{1:n}, \mathbf{X}_{1:n}) d\theta$$

where the predictive distribution explicitly involves both the training data and model parameters (trees and leaf means in the case of BART). In this sense, the proposed approach does "use the data twice", but not in the construction of the posterior. Rather, our procedure is a way of combining the orthodox BART posterior with an intentionally and explicitly distinct posterior predictive model for extrapolation points. Although this is an uncommon approach that violates so-called "diachronic coherence", it is in no sense illicit in that it merely amounts to specifying a user-defined predictive distribution that takes BART posterior samples as inputs. From this perspective, describing the method amounts to providing a definition of the predictive kernel, $f(\tilde{y} \mid \theta, y_{1:n}, \mathbf{X}_{1:n})$. Specifically, this will be a Gaussian process with a covariance kernel defined in terms of the trees of the BART model.

3.1 Notation

Consider a fitted BART forest $\{\widehat{\mathbf{T}}_l \mid 1 \leq l \leq L\}$ with L trees. Let $\{\mathcal{A}_{l1}, \cdots, \mathcal{A}_{lB_l}\}$ denote the covariate space partitioned by the l-th tree $\widehat{\mathbf{T}}_l$ with B_l leaf nodes, and $\widehat{\sigma}^2$ for the estimated residual variance. For the l-th tree, suppose the test point \mathbf{x} falls in a leaf node b with covariate space \mathcal{A}_{lb} . Let the training data that falls in this leaf node and its residuals at the current tree (defined by Equation (2.4)) be noted as \mathbf{X}^{tr} and \mathbf{r}^{tr} . Similarly, \mathbf{X}^{te} and \mathbf{r}^{te} denote the exterior testing data in the leaf node b and its to-be-predicted residuals.

Note that the tree partitioned leaf node \mathcal{A}_{lb} can extend to infinity if they are at the boundary. Specifically, the range of subset of training data \mathbf{X}^{tr} falling in the b-th leaf node of the l-tree forms a p-dimensional hypercube \mathcal{B}_{lb} , which is a subset of \mathcal{A}_{lb} . If the testing point x falls within the range of training data, i.e., $\mathbf{x} \in \mathcal{B}_{lb}$, we consider it as an interior point, and its prediction follows the standard XBART model. Otherwise, if $\mathbf{x} \in \{\mathcal{A}_{lb} \setminus \mathcal{B}_{lb}\}$, it is an exterior point and their predictions require extrapolation. Notably this definition is local, a testing data can be exterior for some of the trees and interior for others in the XBART forest.

3.2 Defining the GP model

To extrapolate the prediction of XBART, we assume that the exterior testing data \mathbf{X}^{te} and training data \mathbf{X}^{tr} in the same leaf node form a Gaussian process. The joint distribution of the training and testing data in a leaf node is given by

$$\begin{pmatrix} \mathbf{r}^{\text{te}} \\ \mathbf{r}^{\text{tr}} \end{pmatrix} \sim N \begin{pmatrix} \mathbf{\Sigma}_{\mathbf{X}^{\text{te}}\mathbf{X}^{\text{te}}}, & \mathbf{\Sigma}_{\mathbf{X}^{\text{te}}\mathbf{X}^{\text{tr}}} \\ \mathbf{\Sigma}_{\mathbf{X}^{\text{tr}}\mathbf{X}^{\text{te}}}, & \mathbf{\Sigma}_{\mathbf{X}^{\text{tr}}\mathbf{X}^{\text{tr}}} + \frac{1}{L}\widehat{\sigma}^{2}\mathbf{I} \end{pmatrix}$$
(3.1)

where μ is the leaf parameter, J is a column vector of ones, and I is an identity matrix. By definition, the variance of the response y is assumed to be σ^2 . Here we assume that the residuals in each tree contribute equally to the total variance.

To reflect the relative distance among covariates, we define the covariance function of the Gaussian process as the squared exponential kernel

$$k(\mathbf{x}, \mathbf{x}') = \tau \exp\left(-\theta \sum_{i=1}^{p} \frac{(x_i - x_i')^2}{2\delta_i^2}\right)$$
(3.2)

where δ_i is the range of the *i*-th variable x_i in a leaf node, θ controls the smoothness and τ determines the scale of the function. $\mathbf{x} = (x_1, \dots, x_p)$ and $\mathbf{x}' = (x_1', \dots, x_p')$ are the vector of two data points. In our experiments, we use $\theta = 0.1$ and set τ to be the variance of observed responses divided by the number of trees.

The conditional distribution of the residuals r^{te} is given by

$$\mu_{\mathbf{X}^{\text{te}}|\mathbf{X}^{\text{tr}}} = \mu \mathbf{J} + \mathbf{\Sigma}_{\mathbf{X}^{\text{te}}\mathbf{X}^{\text{tr}}} \left[\mathbf{\Sigma}_{\mathbf{X}^{\text{tr}}\mathbf{X}^{\text{tr}}} + \frac{1}{L} \widehat{\sigma}^{2} \mathbf{I} \right]^{-1} (\mathbf{r}^{\text{tr}} - \mu \mathbf{J})$$

$$\mathbf{\Sigma}_{\mathbf{X}^{\text{te}}|\mathbf{X}^{\text{tr}}} = \mathbf{\Sigma}_{\mathbf{X}^{\text{te}}} - \mathbf{\Sigma}_{\mathbf{X}^{\text{te}}\mathbf{X}^{\text{tr}}} \left[\mathbf{\Sigma}_{\mathbf{X}^{\text{tr}}\mathbf{X}^{\text{tr}}} + \frac{1}{L} \widehat{\sigma}^{2} \mathbf{I} \right]^{-1} \mathbf{\Sigma}_{\mathbf{X}^{\text{tr}}\mathbf{X}^{\text{te}}}.$$
(3.3)

The prediction for the residuals of the exterior testing data associated with this leaf node is drawn from the conditional normal distribution $\mathbf{r}^{\text{te}} \sim N(\mu_{\mathbf{X}^{\text{te}}|\mathbf{X}^{\text{tr}}}, \mathbf{\Sigma}_{\mathbf{X}^{\text{te}}|\mathbf{X}^{\text{tr}}})$ rather than the fixed leaf parameter of the tree, which is used for predicting interior points.

3.3 Algorithms

It can be computational intensive to find the corresponding training data and calculate the covariance matrix for each test data observation. Following the fast algorithm GrowFromRoot introduced in He et al. (2019), we propose an efficient method that pinpoints the exterior testing data and its neighborhood training data in the same leaf node by recursively partitioning the training and testing data at the same time. The procedures are summarized in Algorithm 1 and 2.

Certain algorithm design choices to boost performance and efficiency are worth emphasizing. First, we partition the covariates into split variables v and active variables v_b . Split variables are those appearing along the decision path from the root to a leaf node. Active variables v_b are a subset of split variables that satisfies the following condition: If there exists a testing point $x \in X^{te}$ such that x is outside the range of \mathcal{B}_{lb} on that variable in leaf node b, then it is considered an active variable. Using only active variables in defining the GP covariance matrix ensures that the extrapolation only depends on those variables, which is both intuitive and improving time efficiency. Second, when the training data sample size is large, we subsample training data when performing the GP extrapolation. Third, to avoid the identification of exterior points being misled by any outliers, we define the hypercube \mathcal{B}_{lb} in each leaf node by the 95% quantile of the training data.

Algorithm 1 Prediction by GP extrapolation

```
1: procedure PREDICT(\mathbf{X}^{\text{te}}, \mathbf{X}^{\text{tr}}, \mathbf{y}_{\text{tr}}, \{\mathbf{T}_{sl}\}, \{\mu_{sl}\}, L, S)
 2: output S Monte Carlo draws of predicted mean \{\widehat{y}_s^{\text{te}}\} for input data \mathbf{X}^{\text{te}}
              Create empty vectors \{\mathbf{r}_{sl}^{\text{tr}}\} and \{\mathbf{r}_{sl}^{\text{te}}\} to store the predicted residuals.
              \mathbf{r} \leftarrow \mathbf{y} - \bar{\mathbf{y}}
  4:
                                                                                                   \triangleright Initialize full residuals for training set X.
              \mathbf{r}_{0l}^{\mathrm{tr}} \leftarrow \bar{\mathbf{y}}/L
                                                                                 ▷ Initialize predicted residuals for the first iteration.
 5:
 6:
              for s in 1 to S do
 7:
                     for l in 1 to L do
                            Create an empty vector v to store split variables.
 8:
                           \begin{split} \mathbf{r} \leftarrow \mathbf{r} - \mathbf{r}_{s-1,l}^{\mathrm{tr}} \\ \mathrm{PFR} \big( \mathbf{r}, \mathbf{X}^{\mathrm{tr}}, \mathbf{r}_{sl}^{\mathrm{tr}}, \mathbf{X}^{\mathrm{te}}, \mathbf{r}_{sl}^{\mathrm{te}}, \mathbf{T}_{sl}, \mu_{sl}, \mathbf{v}, \texttt{root\_node} \big) \end{split}
 9:
                                                                                                                                    ▶ Update partial residuals.
10:
                                                                                                                                                  \triangleright Call Algorithm 2.
                            r \leftarrow r + r_{sl}^{tr}
                                                                                                                                           ▶ Update full residuals.
11:
                     end for
12:
                    \hat{\mathbf{y}}_s^{\text{te}} \leftarrow \sum_{l=1}^L \mathbf{r}_{sl}^{\text{te}}
                                                                                   \triangleright Calculate predicted mean from the s-th iteration.
13:
              end for
14:
              Return predicted means \{\hat{y}_s^{\text{te}}\}.
15:
16: end procedure
```

3.4 Simulation studies

This section compares XBART-GP with various prediction inference methods in regression modeling. Specifically, we compare our proposed method with the original XBART, Jackknife+ and its cross-validation version (CV+) combined with XBART and Random Forest.

For both XBART and XBART-GP, we use the following hyperparametes num_trees = 20, num_iterations = 100, Nmin = 20, $\tau = \text{Var}(y)/\text{num_trees}$ (where Var(y) is the variance of the response variable in the training set). We choose $\theta_{gp} = 0.1$ and $\tau_{gp} = \tau$ to be the smoothness and scale parameters of the kernel function for XBART-GP.

When applying Jackknife+ and CV+ to XBART, we pick the same number of trees and τ value, except that the number of iterations is reduced to 100 to reduce the running time of the two approaches. For simulations of Jackknife+ and CV+ on Random Forest, called Jackknife+ RF and CV+ RF in the rest of the paper, we use the default settings provided in the scikit-learn (Pedregosa et al., 2011) package in Python.

The real signal is drawn from four challenging functions, f, listed in Table 1. The response variable y is generated independently from $y = f(\mathbf{x}) + \epsilon$ with Gaussian noise ϵ . In all cases, we generate 200 data points with covariates $x_j \stackrel{\text{iid}}{\sim} N(0,1)$ for $j=1,\ldots,d=10$ as the training set and another 200 data points with $x_j \stackrel{\text{iid}}{\sim} N(0,1.5^2)$ as the testing set.

Since the definition of exterior point for XBART-GP depends on the tree's structure and varies by leaf nodes, we simplify the concept in this section to evaluate performance on in- and out-of-range data. In our simulation studies, we consider any testing data outside the training data range as exterior points. Under the above settings, approximately half of the testing data is interior, and half is exterior. The performance is then reported on interior and exterior points separately. We repeat the experiments on

Algorithm 2 PredictFromRoot

```
1: procedure PFR(\mathbf{r}, \mathbf{X}^{tr}, \mathbf{r}^{tr}, \mathbf{X}^{te}, \mathbf{r}^{te}, T_l, \mu_l, \mathbf{v}, node)
 2: \mathbf{outcome} Predict residuals \mathbf{r}^{te} for testing covariates \mathbf{X}^{te} using Gaussian process.
             if node is leaf node then
                    Define hypercube \mathcal{B}_{lb} based on the range of \mathbf{X}^{tr}.
 4:
                    Define active variables v_b based on \mathbf{X}^{\text{te}} and \mathcal{B}_{lb}.
                                                                                                                       ▶ If there exists a testing point
 5:
       x \in X^{te} such that x is out of the range of \mathcal{B}_{lb} on that variable, then it is considered as an
       active variable.
                    Sample a subset of training data \mathbf{X}_b^{\mathrm{tr}} and \mathbf{r}_b^{\mathrm{tr}} of size 100 with only variables in \mathbf{v}_b.
 6:
                    Get exterior testing data \mathbf{X}_b^{\text{te}} with only variables in \mathbf{v}_b.
 7:
                    Get covariance matrix \Sigma_{\mathbf{X}_{h}^{\text{tr}}\mathbf{X}_{h}^{\text{tr}}} and its inverse \Sigma_{\mathbf{X}_{h}^{\text{tr}}\mathbf{X}_{h}^{\text{tr}}}^{-1} for the Gaussian process.
 8:
                    Get conditional mean and variance \mu_{\mathbf{X}_{h}^{\text{te}}|\mathbf{X}_{h}^{\text{tr}}}, \sigma_{\mathbf{X}_{h}^{\text{te}}|\mathbf{X}_{h}^{\text{tr}}} from Equation (3.3).
 9:
                    \mathbf{r}^{\mathrm{tr}} \leftarrow \mu_{lb}
10:
                                                                                   \triangleright Assign leaf parameter \mu_{lb} as predicted residuals.
       \mathbf{r}_b^{\mathrm{te}} \leftarrow \boldsymbol{\mu}_{\mathbf{X}_b^{\mathrm{te}} | \mathbf{X}_b^{\mathrm{tr}}} + \boldsymbol{\Sigma}_{\mathbf{X}_b^{\mathrm{te}} | \mathbf{X}_b^{\mathrm{tr}} \mathbf{Z}} \\ \text{vector of standard normal variables}.
                                                                                  ▷ Sample predictions from Gaussian process; z is a
11:
                    for i in 1 to N_t do
                                                                                                         \triangleright N_t is the number of the testing data.
12:
                           if \mathbf{X}^{\text{te}}[i] \in \mathcal{B}_{lb} then
13:
                                 \mathbf{r}^{\text{te}}[i] \leftarrow \mu_{lb}
                                                                                            ▶ Assign leaf parameter as predicted residual.
14:
15:
                                                                                         ▶ Assign prediction from the Gaussian process.
16:
                           end if
17:
                    end for
18:
             else
                                                                                                                     ▷ Split until reaching leaf nodes.
19:
                    Get split variable v and cutpoint c. Add v to splitting variables v.
20:
                    Shift r, \mathbf{X}^{tr}, r^{tr}, \mathbf{X}^{te}, r^{te} into left and right parts according to v and c.
21:
                    	ext{PFR}\Big(	ext{r}_{	ext{left}}, \mathbf{X}_{	ext{left}}^{	ext{tr}}, \mathbf{r}_{	ext{left}}^{	ext{tr}}, \mathbf{X}_{	ext{left}}^{	ext{te}}, \mathbf{r}_{	ext{left}}^{	ext{te}}, T_l, \mu_l, 	ext{v}, 	ext{left\_node}\Big)
22:
                    \mathrm{PFR}\Big(\mathrm{r}_{\mathrm{right}},\mathbf{X}_{\mathrm{right}}^{\mathrm{tr}},\mathrm{r}_{\mathrm{right}}^{\mathrm{tr}},\mathbf{X}_{\mathrm{right}}^{\mathrm{te}},\mathrm{r}_{\mathrm{right}}^{\mathrm{te}},\mathrm{r}_{\mathrm{right}}^{\mathrm{te}},T_{l},\mu_{l},\mathrm{v},\mathtt{right\_node}\Big)
23:
24:
             end if
25: end procedure
```

Name	Function
Linear	$x^t \gamma; \ \gamma_j = -2 + \frac{4(j-1)}{d-1}$
Single index	$10\sqrt{a} + \sin(5a)$; $a = \sum_{j=1}^{10} (x_j - \gamma_j)^2$; $\gamma_j = -1.5 + \frac{j-1}{3}$.
Trig + poly	$5\sin(3x_1) + 2x_2^2 + 3x_3x_4$
Max	$\max(x_1, x_2, x_3)$

Table 1: Four true f functions

each data generating process 10 times and calculate the average empirical probability of coverage and the average interval length with coverage level $1 - \alpha = 0.9$.

Simulation studies and time efficiency comparison on XBART-GP and its baselines were conducted in Python 3.8.10 on a Linux machine with Intel(R) Core(TM) i7-8700K CPU @ 3.70GHz processor and 64GB RAM; eight cores were used for parallelization whenever it was applicable.

Figure 3 visualizes the simulation results on linear and single index functions. The

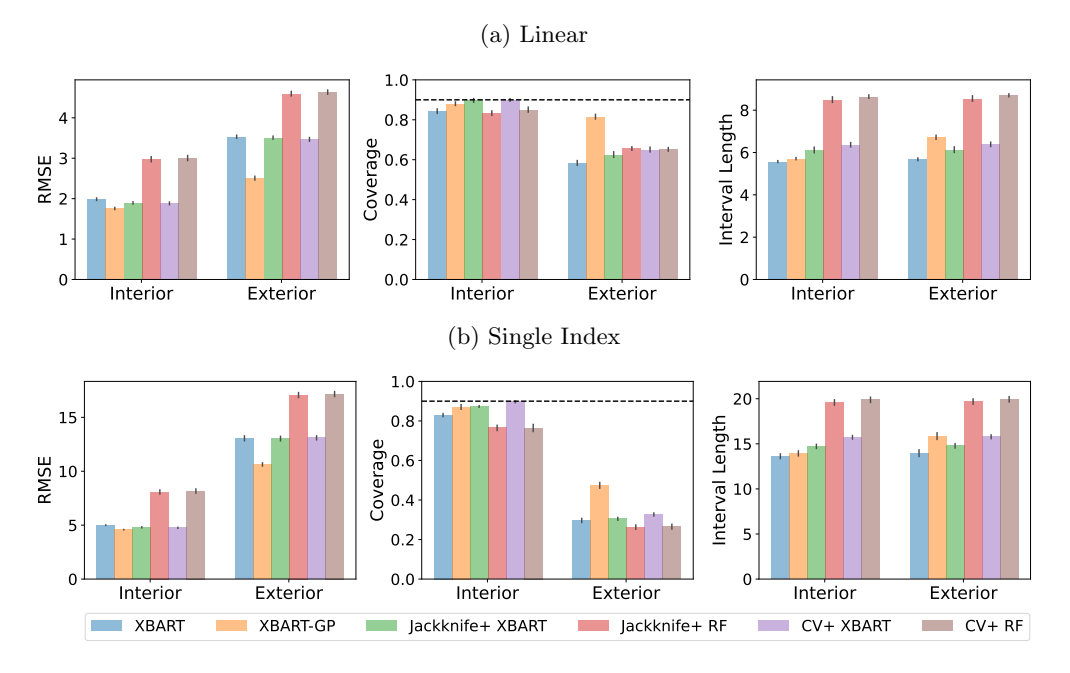


Figure 3: Visualization of simulation results in root mean square error (RMSE), interval coverage (Coverage), and interval length for interior and exterior points for linear and single index functions. The horizontal dash line indicates the 90% target coverage level.

full results of four functions are summarized in the Appendix Figure 7 and Table 3. This figure compares the root mean square error (RMSE) of point prediction, coverage rate, and interval length of various approaches. Note that the RMSE of Jackknife+ and CV+ are evaluated based on the average leave-one-out prediction and cross-validated prediction, respectively.

We notice that XBART-GP has the smallest RMSE of point prediction across all functions on both interior and exterior points. For interior data, our approach is the only one that delivers nominal coverage while the interval length is not too large. Furthermore, it also has substantially greater prediction coverage than the baseline methods on exterior points. It is worth noting that XBART-GP achieves better coverage without inflating the prediction interval too much. Indeed, the interval length of XBART-GP is just slightly larger than that of Jackknife+XBART or CV+XBART but is still smaller than that of Jackknife+RF or CV+RF.

Combining Jackknife+ and CV+ with XBART, the two methods produce competitive RMSE, coverage, and interval length compared to XBART itself on interior points. However, the prediction inference methods also fail to extrapolate as the in-sample residuals can not inform uncertainty on out-of-range data.

Time efficiency comparison

We then evaluate the performance and time efficiency of XBART-GP and other baselines for increasing sample size.

The training and testing covariates are generated from the same distributions as in the previous section, with testing covariates having a slightly larger variance. We generate the response variable Y with the linear function in Table 1 and the standard normal error term. We estimate the average coverage, interval width and computational time of all 6 methods on with sample size $n = n_t = 50, 100, 150, 200, 300, 500$ over 10 independent trials for each sample size. The target coverage level is $1 - \alpha = 0.9$.

Figure 4 illustrates the performance comparison of XBART-GP and other baseline methods on exterior points with an increasing sample size. The performance on interior points is similar and is presented in Appendix Figure 8. Note that the proportion of exterior points generated varies according to the training size. Empirically, the percentage of exterior points decreases from 80% to 40% when the sample size increases from 50 to 500 on 10-dimensional covariates. The x-axises in Figure 4 only reflect the sizes of the training sets. The running time is reported as evaluating all testing data, including interior and exterior points.

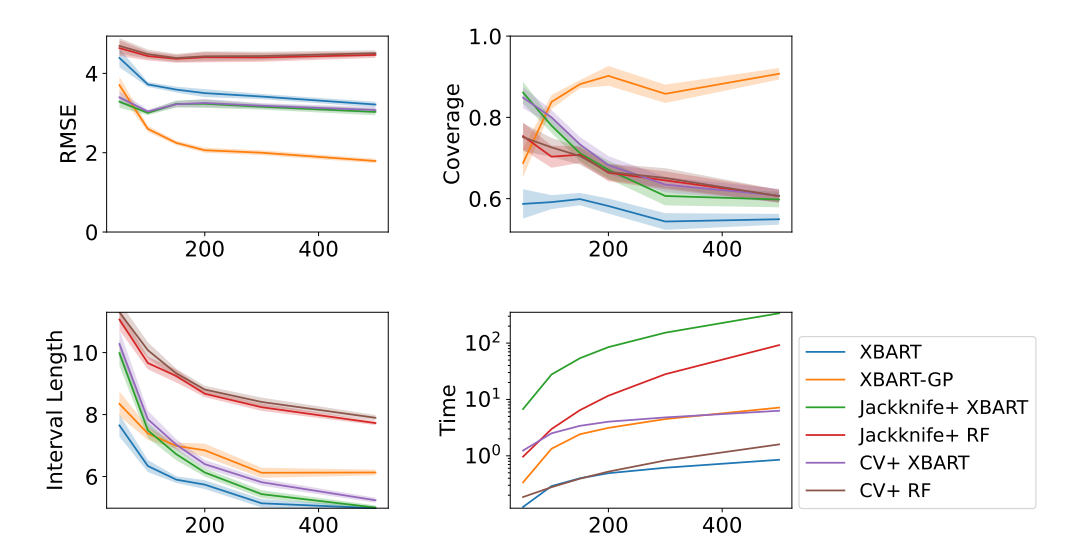


Figure 4: Average RMSE, coverage, interval length on exterior points, and running time (in seconds) at 90% level for all methods over 10 independent trials with increasing sample size from 50 to 500. Time in seconds is presented in logarithm scale.

On exterior points, XBART-GP has the smallest RMSE of point prediction and a stable coverage close to 90% as the sample size grows. The coverage of other baseline methods drops significantly on a larger sample size. The interval of XBART-GP is slightly wider than XBART but still outperforms random forest approaches.

XBART and CV+ approaches are the most efficient in terms of running time. The run-time of XBART-GP increases almost linearly with the amount of training and testing sample size, but it is worth the time when the distribution of the test set shifts from the training set.

4 Local GP extrapolation with Bayesian causal forests

As stated in Section 2.5, one of the crucial assumptions in causal inference is the positivity assumption, also known as the overlap assumption. Violation of the positivity assumption can lead to substantially biased treatment effect estimates. In this section we describe how to apply the tree-based Gaussian process approach to the XBCF model (Krantsevich et al., 2022) to address the non-overlap problem (hereafter XBCF-GP). Certain modifications of the procedure are necessary due to the fact that the extrapolation of interest is on the treatment effect function, which is a difference of two response surfaces.

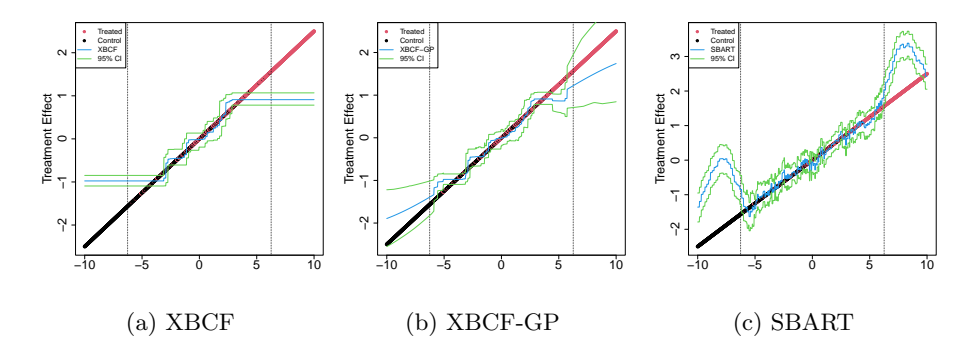


Figure 5: An example of treatment effect estimation with positivity violation. Black points indicate treated units and red points indicate control units. The XBCF (Left), XBCF-GP (Middle), and SBART (Right) estimations are in blue lines and their 95% confidence interval are the green lines. The two vertical dashed lines are the boundary of the overlap area. The traditional Bayesian causal forests estimate the treatment effect in the non-overlap area by a constant of the corresponding leaf node.

Figure 5 is a toy example of the treatment effect estimation on simulation data with positivity violation. We illustrate the extrapolation ability by applying local Gaussian process to Bayesian causal forests. It is compared to the original XBCF method and one alternative extrapolation technique, called SBART, which will be introduced in the following simulation section.

The treatment trees in the XBCF model stop splitting when the amount of treated or control data is small in a leaf node, yielding a constant and biased estimation of the treatment effect for all data in the non-overlap area. On the other hand, the extrapolation of SBART lacks regularization and heavily relies on the shape of the prognostic

function. In addition, the 95% confidence intervals of the two methods stay tight for the conditional treatment effect in the non-overlap region. Extrapolating the XBCF estimates using the local Gaussian process allows it to estimate the non-overlap treatment effect directionally and provide appropriate inference as the data deviates from the overlap region (to a degree depending on the user-defined Gaussian process covariance parameters).

To apply the Gaussian process extrapolation to the XBCF model, we make some adjustments to both the GP algorithm introduced in the previous section and the XBCF algorithm. First, we formally define the overlap and non-overlap area in the ensemble trees framework. Then we explain how to apply the algorithms introduced in XBART-GP to extrapolate the treatment effect.

Given a regression tree, consider a leaf node b with local covariate subspace $\mathcal{A}_{\mathbf{X}}$, let matrix \mathbf{X}^{tr} denote the training data that falls into the leaf node, which can be separated into a treatment group $\mathbf{X}_{T}^{\mathrm{tr}}$ and a control group $\mathbf{X}_{C}^{\mathrm{tr}}$ based on the corresponding treatment variable z. The range of covariates in the treated and the control form two hypercubes, here we denote as \mathcal{B}_{T} and \mathcal{B}_{C} respectively. The overlap region in the leaf node is the intersection of \mathcal{B}_{T} and \mathcal{B}_{C} , or $\mathcal{B}_{O} = \mathcal{B}_{T} \cap \mathcal{B}_{C}$. Consequently, the non-overlap area is $\mathcal{B}_{NO} = \mathcal{A}_{\mathbf{X}} \setminus \mathcal{B}_{O}$.

Notably, in each treatment tree, the residuals in the non-overlap area are directionally biased relative to the true treatment effect, due to the no-splitting behavior of the treatment trees, and will extrapolate any testing data into the opposite direction if included in the Gaussian process. Therefore, different from XBART-GP, we assume that the testing data in the non-overlap area $\mathbf{X}_{\mathrm{NO}}^{\mathrm{te}}$ share a joint distribution with only the overlap training data $\mathbf{X}_{\mathrm{O}}^{\mathrm{tr}}$, namely

$$\begin{pmatrix} \mathbf{r}_{\mathrm{NO}}^{\mathrm{te}} \\ \mathbf{r}_{\mathrm{O}}^{\mathrm{tr}} \end{pmatrix} \sim N \left(\mu \mathbf{J}, \begin{pmatrix} \mathbf{\Sigma}_{\mathbf{X}_{\mathrm{NO}}^{\mathrm{te}}} \mathbf{X}_{\mathrm{NO}}^{\mathrm{te}}, & \mathbf{\Sigma}_{\mathbf{X}_{\mathrm{NO}}^{\mathrm{te}}} \mathbf{X}_{\mathrm{O}}^{\mathrm{tr}} \\ \mathbf{\Sigma}_{\mathbf{X}_{\mathrm{O}}^{\mathrm{tr}}} \mathbf{X}_{\mathrm{NO}}^{\mathrm{te}}, & \mathbf{\Sigma}_{\mathbf{X}_{\mathrm{O}}^{\mathrm{tr}}} \mathbf{X}_{\mathrm{O}}^{\mathrm{tr}} + \frac{1}{L} \widehat{\boldsymbol{\sigma}}_{\mathbf{z}}^{2} \end{pmatrix} \right). \tag{4.1}$$

Here $\mathbf{r}_{\mathrm{O}}^{\mathrm{tr}}$ is a vector of partial residuals for the current treatment tree, i.e., the difference between observed response y and the predictions of all other prognostic and treatment trees. $\mathbf{r}_{\mathrm{NO}}^{\mathrm{te}}$ is a vector of residuals we wish to predict for the non-overlap testing data. $\hat{\boldsymbol{\sigma}}_{\mathrm{z}}^{2}$ is a diagonal matrix with diagonal elements equal to estimated variance $\hat{\sigma}_{0}^{2}$ or $\hat{\sigma}_{1}^{2}$ depending on the treatment variable of the training data and L is the total number of prognostic and treatment trees.

The prediction algorithm for the treatment trees in XBCF-GP follows the same procedures as in Algorithm 2 except for the difference we describe above. Specifically, we replace the out-of-range hypercube \mathcal{B}_{lb} in line 4 by the overlap area \mathcal{B}_O . In line 6, the subset of training data \mathbf{X}_b^{tr} is sampled from the training data \mathbf{X}_O^{tr} from the overlap area instead of the entire training set. Then in line 7, we choose to extrapolate the testing data $\mathbf{X}_{NO}^{\text{te}}$ in the non-overlap area for XBCF-GP. Similar to the algorithm design choices made in XBART-GP, the overlap area is defined by the 95% quantiles of the treated and control data for robustness concerns.

In addition to the modification we make to the XBART-GP algorithms, we also add a tweak to the original XBCF model to ensure the extrapolation works smoothly. In

particular, the GP extrapolation requires a minimum amount of overlap data in the leaf node to provide informative estimates. Though the treatment trees in XBCF are unlikely to split in the non-overlap area, it could happen on rare occasions and lead to poor extrapolation performance. Thus, we add a strong prior on the treatment trees such that any split rule that does not have enough treatment and control data in the children nodes will receive zero likelihood to be split on. The amount of overlap data required in a leaf node is controlled by the hyperparameter Nmin. It is a sensitive parameter that leverages how well the method performs near the boundary in the overlap area versus its extrapolation in the non-overlap region. In our experiments with 500 data points, we choose Nmin = 20.

The mixed model XBCF-GP combines the advantages of the Bayesian causal forest and the Gaussian process. The XBCF component can accurately and efficiently estimate homogeneous and heterogeneous treatment effects on large datasets with high-dimensional covariates under positivity assumption. The Gaussian process on the leaf node level enables extrapolation of the treatment effect in the non-overlap region using the most relevant covariates in the neighborhood.

Our approach is a better way to characterize the uncertainty of the estimated treatment effect for positivity violations. Specifically, our uncertainty estimation, defined by the covariate function of the Gaussian process, reflects the distance between the testing data and the overlap region. If the testing data lies far away from it, XBCF-GP will reflect such uncertainty in terms of wider prediction intervals.

4.1 Simulation study

This section demonstrates the comparison of prediction interval coverage and length under the setting of causal inference when the positivity assumption is violated. To demonstrate the performance of XBCF-GP, we compare it with a set of alternative extrapolation approaches proposed by Nethery et al. (2019). The baseline methods we use are summarized as follows:

- **SBART** Also known as BART-Stratified. Fit separate BART models for the treated and the control group, then estimate the treatment effect as the difference between the expected value of the treated and the control models.
- **UBART** Untrimmed BART is implemented by Nethery et al. (2019), in which a single BART model is fitted with covariates, treatment variable, and estimated propensity score. The treatment effect is estimated by predicting the potential outcomes with the posterior predictive distributions.
- BART+SPL Nethery et al. (2019) proposed this method to estimate the overlap area with BART and the non-overlap area with a spline model. The region of overlap is defined by propensity score with recommended parameters a = 0.1 and b = 7.

Figure 6 illustrates the performance of XBCF-GP and other baseline methods on a one-dimensional toy dataset. The independent variable x is uniformly drawn from the

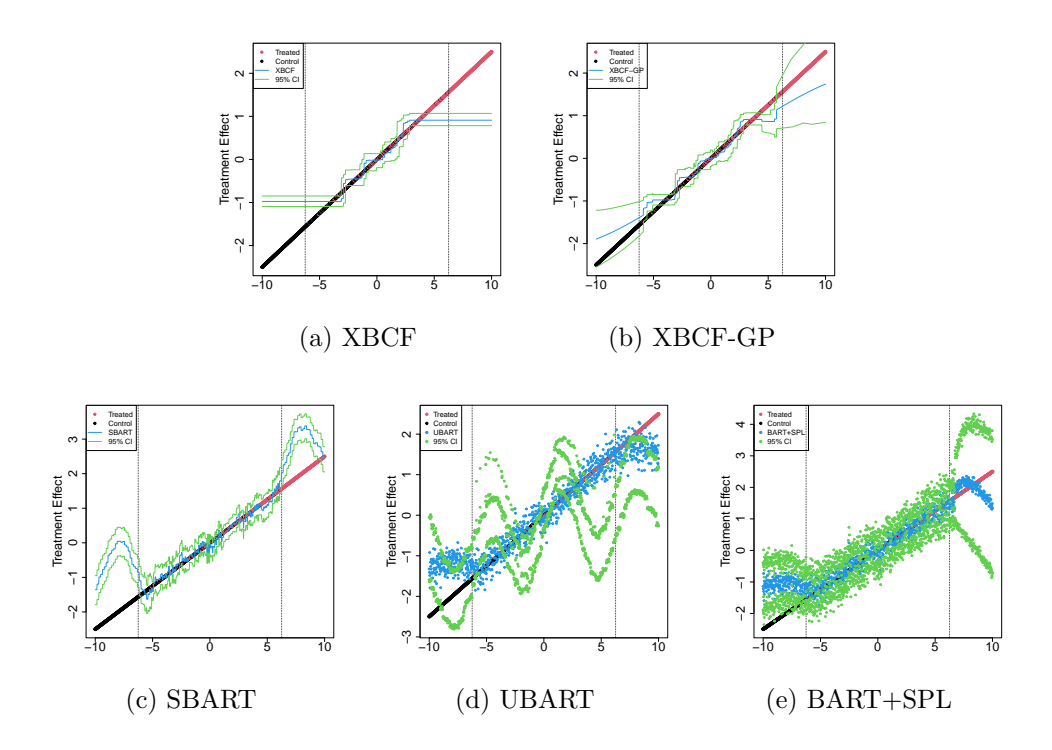


Figure 6: An example of treatment effect estimation with positivity violation on all baseline methods. Black points indicate treated units and red points indicate control units. The estimated treatment effects are in blue lines and their 95% confidence interval are the green lines. The two vertical dashed lines are the boundary of the overlap area.

range [-10, 10]. The prognostic function is sine and the treatment effect is 0.25x. The probability for a sample being treated is $\pi(x) = \max\{0, \min\{1, 0.08x + 0.5\}\}$. Let $f(x) = \sin(x) + (0.25x)z$ denotes the true function with treatment variable $z \sim \text{Bern}(\pi(x))$. The response values y are generated as $y = f(x) + \epsilon$, where $\epsilon \sim N(0, 0.2 \times \text{sd}(f))$ with the standard deviation sd(f) taken over the dataset. The fitted models in the example use the same parameter set-up as in the simulation study, which will be specified shortly.

The example clearly showcases the behavior of different models in terms of conditional average treatment effect estimation. The first three methods (XBCF, XBCF-GP, and SBART) are robust to the noise. The latter two methods (UBART and BART+SPL) use the response variable directly to estimate CATE, thus introducing large noises in the estimators. The prognostic structure easily influences the CATE estimations of all three BART-based methods, especially in the non-overlap area. XBCF dodges the bullet by setting up a separate BART forest to control for the prognostic effect, but it cannot extrapolate properly in positivity violation. XBCF-GP inherits the well-regularized structure from XBCF and extrapolates the treatment effect estimations nice and smoothly.

For a more thorough comparison among these methods, we adopt the same data generating process used in Hahn et al. (2020) and Krantsevich et al. (2022) but modify the propensity function to create the positivity violation scenario. The covariate vector x consists of five variables. The first three (denoted as x_1, x_2, x_3) are generated from the standard normal distribution. x_4 is a binary variable, and x_5 is an unordered categorical variable with levels denoted as 1, 2, 3. The prognostic function can be either linear or nonlinear:

$$\mu(\mathbf{x}) = \begin{cases} 1 + g(x_4) + x_1 x_3 & \text{linear} \\ -6 + g(x_4) + 6|x_3 - 1| & \text{nonlinear,} \end{cases}$$

where g(1) = 2, g(2) = -1 and g(3) = -4. The treatment effect can be either homogeneous or heterogeneous:

$$\tau(\mathbf{x}) = \begin{cases} 3 & \text{homogeneous} \\ 1 + 2x_2x_5 & \text{heterogeneous.} \end{cases}$$

In our simulation, we adjust the propensity function such that roughly 20% of the data has a propensity score of 1, 20% of the data has a propensity score of 0, and the rest of the data has a propensity score that is between 0 and 1. The propensity function $\pi(x)$ is given by

$$\pi(\mathbf{x}) = \max\{0, \min\{1, h(\mathbf{x})\}\}, \quad h(\mathbf{x}) = 1.1\Phi(3\mu(\mathbf{x})/s - 0.5x_1 - c) - 0.15 + u_i/10,$$
 (4.2)

where s is the standard deviation of $\mu(\mathbf{x})$ taken over the observed samples and $u_i \sim \text{Uniform}(0,1)$. We pick the value c=0 for linear prognostic function and c=3 for the non-linear one. For any propensity score greater than 1 or less than 0, we set it to be 1 or 0, respectively. In addition, we add a Gaussian noise $\epsilon \sim N(0, 0.5 \times \text{sd}(\mu(\mathbf{x}) + \tau(\mathbf{x})\mathbf{z}))$ with the standard deviation taken over the samples to generate the response values.

To gauge the performance of XBCF-GP across overlap and non-overlap regions, we evaluate the average treatment effect (ATE) and conditional average treatment effect (CATE) on three basic metrics: average root mean square error, coverage, and average interval length. In addition, we also compare the time efficiency of the proposed method to baseline methods. We average the results from 20 independent replications for each scenario with n=500 samples.

For methods that rely on propensity score, we use the propensity score estimated by a XBART Multinomial model with 2 classes and 100 iterations instead of the true propensity scores. For XBCF-GP, we set hyper-parameter $\theta=0.1$ and $\tau=\widehat{\sigma}^2/L_{\tau}$, where $\widehat{\sigma}^2$ is the estimated variance and $L_{\tau}=20$ is the default number of treatment trees in the XBCF model. We choose a different scale parameter τ_{gp} from XBART-GP as the variance of the treatment effect tends to be smaller than the total variance of the observed data in most cases. As for the other baseline methods including XBCF, we use their default parameters for all scenarios.

To compare with the baseline methods, the experiments were conducted in R 4.1.3 on the same machine as described in the previous sections. Parallelization was used whenever it was applicable.

Method	ATE			CATE					
	RMSE	Coverage	I.L.	RMSE	Coverage	I.L.	Time		
Linear Homogeneous									
XBCF	0.446	0.700	0.958	0.514	0.876	1.650	0.89		
XBCF-GP	0.427	0.700	0.945	0.504	0.895	1.708	2.84		
SBART	1.089	0.050	0.942	1.478	0.755	3.286	7.32		
UBART	0.400	0.800	1.181	1.341	0.993	5.808	6.58		
BART+SPL	0.903	0.950	3.602	1.629	0.986	13.759	84.24		
Linear Heterogeneous									
XBCF	0.681	0.750	1.501	1.672	0.804	3.798	0.89		
XBCF-GP	0.634	0.750	1.586	1.560	0.825	3.977	5.47		
SBART	1.184	0.050	1.461	1.839	0.878	5.438	7.31		
UBART	0.492	0.950	1.913	2.167	0.838	8.797	6.61		
BART+SPL	1.501	0.950	7.204	3.158	0.943	23.702	87.81		
Non-linear Homogeneous									
XBCF	0.603	0.850	2.135	0.574	0.957	2.766	0.83		
XBCF-GP	0.563	0.850	2.304	0.545	0.972	3.088	3.01		
SBART	2.359	0	2.535	3.416	0.805	7.822	7.33		
UBART	0.488	1	2.626	2.819	0.918	12.921	6.59		
BART+SPL	1.476	1	6.999	3.531	0.989	25.728	88.30		
Non-linear Heterogeneous									
XBCF	0.976	0.850	2.502	2.416	0.766	5.160	0.85		
XBCF-GP	0.955	0.800	2.592	2.336	0.792	5.700	4.93		
SBART	2.761	0	2.758	3.924	0.804	8.843	7.36		
UBART	0.596	0.950	2.922	3.182	0.830	13.946	6.59		
BART+SPL	2.191	0.900	8.815	4.459	0.957	29.450	89.75		

Table 2: Results of root mean square error (RMSE), interval coverage (Coverage), interval length (I.L.), and running time (in seconds) for ATE and CATE estimators with different combinations of treatment term and prognostic term types. The sample size is 500.

Table 2 summarizes the simulation results of various methods. We focus our discussion here on CATE estimation. Both XBCF methods provide the best CATE estimation in all cases and deliver competitive CATE coverage with tighter intervals than other methods. XBCF-GP is able to improve both the accuracy and coverage of ATE and CATE estimation on the basis of its base model. Furthermore, we notice the efficiency of XBCF-GP, inherited from XBART, is substantially faster than other BART-based methods.

5 Discussion

The Gaussian process extrapolation technique developed here has several advantages over standard BART extrapolation, as implemented in most widely available software. First, whereas BART extrapolates a constant function beyond the range of the training data, by fusing a Gaussian process at each leaf, "local" Gaussian process extrapolation

is possible. This local GP approach automatically incorporates variable relevance, using only variables that are used as splitting rules in a given tree. Because extrapolation occurs at each tree, our procedure also improves prediction generally: GP prediction at *local* exterior points imposes additional smoothness even at points that are within the convex hull of the training data.

Second, BART's prediction intervals are dominated by the residual variance parameter value, which implies that the interval width is nearly constant at any exterior point. By contrast, the local GP extrapolation method implies interval widths that expand quite rapidly the further away a point is from the training data, a desirable property that is directly inherited from the Gaussian process.

Third, the local GP approach requires no additional training time compared to a regular BART model fit. Rather, the extrapolation component is a direct modification of the posterior predictive distribution defined in terms of BART posterior samples and a specified covariance function. Broadly, our approach grew out of attempts to answer the question: how would one want to use a known BART model that fit well at interpolation points to define an extrapolation model? Our proposed solution is to graft a Gaussian process to each leaf node for the purpose of extrapolation only; posterior uncertainty in the BART model parameters is then propagated by averaging over posterior samples. The general philosophy behind this approach is that there is no need to change the likelihood model if BART is adequately fitting the training data; but, conversely, there is no need to stick to the pure BART model for points lying far from the training data. Extrapolation always requires a leap of faith and there is no guarantee that any extrapolation method will succeed, but we argue that there are conceptual as well as computational advantages to disentangling the extrapolation model from the interpolation model.

Finally, we demonstrate how to apply local GP extrapolation of BART models to the problem of imperfect overlap in treatment effect estimation, a common practical challenge in applied causal inference. By applying the local GP extrapolation technique to the Bayesian causal forest model, violations of the positivity assumption can be handled organically. Specifically, we are able to extrapolate the treatment effect surface directly rather than composing it as the difference of two separate extrapolations (one for each treatment arm). Our simulation studies demonstrate that XBCF-GP produces treatment effect estimates with good coverage on a variety of data-generating processes. We anticipate that these tools will help other researchers to draw more reliable inferences from applied data which frequently exhibit imperfect overlap.

References

Barber, R. F., Candes, E. J., Ramdas, A., and Tibshirani, R. J. (2021). "Predictive inference with the jackknife+." The Annals of Statistics, 49(1): 486–507. 2, 7, 24

Breiman, L. (2001). "Random forests." Machine learning, 45(1): 5–32. 1

Breiman, L., Friedman, J., Olshen, R., and Stone, C. J. (1984). Classification and regression trees. Chapman and Hall/CRC. 1

- Chen, T. and Guestrin, C. (2016). "XGBoost: A scalable tree boosting system." In Proceedings of the 22nd ACM SIGKDD International Conference on Knowledge Discovery and Data Mining, 785–794. ACM. 1
- Chipman, H. A., George, E. I., McCulloch, R. E., et al. (2010). "BART: Bayesian additive regression trees." *The Annals of Applied Statistics*, 4(1): 266–298. 1, 3, 4, 5
- Crump, R. K., Hotz, V. J., Imbens, G. W., and Mitnik, O. A. (2009). "Dealing with limited overlap in estimation of average treatment effects." *Biometrika*, 96(1): 187–199. 7
- D'Amour, A., Ding, P., Feller, A., Lei, L., and Sekhon, J. (2021). "Overlap in observational studies with high-dimensional covariates." *Journal of Econometrics*, 221(2): 644–654. 3, 7
- Efron, B. and Stein, C. (1981). "The jackknife estimate of variance." The Annals of Statistics, 586–596. 2, 7
- Gramacy, R. B. and Lee, H. K. H. (2008). "Bayesian treed Gaussian process models with an application to computer modeling." *Journal of the American Statistical Association*, 103(483): 1119–1130. 2
- Hahn, P. R., Murray, J. S., Carvalho, C. M., et al. (2020). "Bayesian regression tree models for causal inference: regularization, confounding, and heterogeneous effects." *Bayesian Analysis*. 3, 8, 19
- He, J. and Hahn, P. R. (2021). "Stochastic tree ensembles for regularized nonlinear regression." *Journal of the American Statistical Association*, (just-accepted): 1–61. 1, 5, 8
- He, J., Yalov, S., and Hahn, P. R. (2019). "XBART: Accelerated Bayesian Additive Regression Trees." In The 22nd International Conference on Artificial Intelligence and Statistics, 1130–1138. 5, 10
- Ho, D. E., Imai, K., King, G., and Stuart, E. A. (2007). "Matching as Nonparametric Preprocessing for Reducing Model Dependence in Parametric Causal Inference." Political Analysis, 15(3): 199–236.
- Imbens, G. W. and Rubin, D. B. (2015). Causal inference in statistics, social, and biomedical sciences. Cambridge University Press. 7
- Krantsevich, N., He, J., and Hahn, P. R. (2022). "Stochastic Tree Ensembles for Estimating Heterogeneous Effects." 3, 8, 15, 19
- Li, F., Morgan, K. L., and Zaslavsky, A. M. (2018a). "Balancing Covariates via Propensity Score Weighting." *Journal of the American Statistical Association*, 113(521): 390–400. 8
- Li, F., Thomas, L. E., and Li, F. (2018b). "Addressing Extreme Propensity Scores via the Overlap Weights." American Journal of Epidemiology, 188(1): 250–257. 8
- Nethery, R. C., Mealli, F., and Dominici, F. (2019). "Estimating population average causal effects in the presence of non-overlap: The effect of natural gas compressor

- station exposure on cancer mortality." The annals of applied statistics, 13(2): 1242. 3, 8, 17
- Papadopoulos, H. (2008). Inductive conformal prediction: Theory and application to neural networks. INTECH Open Access Publisher Rijeka. 2, 7
- Pedregosa, F., Varoquaux, G., Gramfort, A., Michel, V., Thirion, B., Grisel, O., Blondel, M., Prettenhofer, P., Weiss, R., Dubourg, V., Vanderplas, J., Passos, A., Cournapeau, D., Brucher, M., Perrot, M., and Duchesnay, E. (2011). "Scikit-learn: Machine Learning in Python." Journal of Machine Learning Research, 12: 2825–2830. 11
- Petersen, M. L., Porter, K. E., Gruber, S., Wang, Y., and van der Laan, M. J. (2012). "Diagnosing and responding to violations in the positivity assumption." *Statistical Methods in Medical Research*, 21(1): 31–54. PMID: 21030422. 7
- Rasmussen, C. E. (2003). "Gaussian processes in machine learning." In Summer school on machine learning, 63–71. Springer. 6
- Vovk, V. (2015). "Cross-conformal predictors." Annals of Mathematics and Artificial Intelligence, 74(1): 9–28. 2, 7
- Yang, S. and Ding, P. (2018). "Asymptotic inference of causal effects with observational studies trimmed by the estimated propensity scores." *Biometrika*, 105(2): 487–493.
- Zhu, Y., Mitra, N., and Roy, J. (2022). "Addressing Positivity Violations in Causal Effect Estimation using Gaussian Process Priors." 3, 8

Acknowledgments

Jingyu He acknowledges support from Hong Kong UGC grant.

Appendix A: Jackknife+ details

For completeness of this paper, we briefly introduce the Jackknife+ (Barber et al., 2021) in this section. Suppose the training set \mathbf{X} consists of n samples of i.i.d training data (\mathbf{x}_i, y_i) , for $i = 1, \ldots, n$, and a new test point \mathbf{x}' to predict. Hereby the subscript -i denotes all data observations except the i-th. Let $\widehat{f} : \mathbb{R}^d \to \mathbb{R}$ denote a fitted regression model on the training set \mathbf{X} . A naive prediction interval of nominal confidence level $1-\alpha$ for the test point \mathbf{x}' is $\widehat{f}(\mathbf{x}') \pm \widehat{q}_{n,\alpha/2}^+\{|y_i-\widehat{f}(\mathbf{x}_i)|\}$. However, note that the residuals $|y_i-\widehat{f}(\mathbf{x}_i)|$ of the training data are often smaller than that of the testing data due to overfitting. Thus this naive method would typically undercover the target level due to underestimation of the residual variance.

The standard Jackknife constructs predictive interval based on the leave-one-out strategy, namely training a fitted model $\hat{f}_{-i}(\mathbf{x})$ by leaving out (\mathbf{x}_i, y_i) for each of n training data at a time. It then obtains n "out-of-sample" residuals $|y_i - \hat{f}_{-i}(\mathbf{x}_i)|$. The prediction interval given by Jackknife is

$$\widehat{C}_{n,\alpha}^{\text{Jackknife}}(\mathbf{x}') = \widehat{f}(\mathbf{x}') \pm \widehat{q}_{n,\alpha/2}^{+}\{|y_i - \widehat{f}_{-i}(\mathbf{x}_i)|\}. \tag{A.1}$$

The Jackknife+ approach differs from the Jackknife by centering the interval on the prediction of leave-one-out models $\hat{f}_{-i}(\mathbf{x})$ instead of the model $\hat{f}(\mathbf{x})$ fitted on the full training data. It inflates variance of prediction, thus achieves better coverage than the naive confidence interval. The prediction interval of Jackknife+ is constructed by

$$\widehat{C}_{n,\alpha}^{\text{Jackknife+}}(\mathbf{x}') = \left[\widehat{q}_{n,\alpha/2}^{-}\{\widehat{f}_{-i}(\mathbf{x}') - |y_i - \widehat{f}_{-i}(\mathbf{x}_i)|\}, \widehat{q}_{n,\alpha/2}^{+}\{\widehat{f}_{-i}(\mathbf{x}') + |y_i - \widehat{f}_{-i}(\mathbf{x}_i)|\}\right],$$
(A.2)

which obtains more rigorous target-level coverage than its predecessor under the assumption that the training and testing data are exchangeable.

Fitting a leave-one-out model for each training data can be computationally expensive, especially for large training size. Barber et al. (2021) also propose a cross-validation version of Jackknife+, named CV+, to tackle this problem. Suppose we split the training data into K subsets, denoted by S_1,\ldots,S_K . Let \widehat{f}_{-S_k} be the fitted model with subset S_k removed. The "out-of-sample" residual for training data \mathbf{x}_i is then given by $r_i^{CV} = |y_i - \widehat{f}_{-S_{k(i)}}(\mathbf{x}_i)|$ where $k(i) \in 1,\ldots,K$ identifies the subset that data point (\mathbf{x}_i,y_i) belongs to. The CV+ prediction interval is defined as

$$\widehat{C}_{n,K,\alpha}^{\text{CV+}}(\mathbf{x}') = \left[\widehat{q}_{n,\alpha/2}^{-}\{\widehat{f}_{-S_{k(i)}}(\mathbf{x}_i) - r_i^{\text{CV}}\}, \widehat{q}_{n,\alpha/2}^{+}\{\widehat{f}_{-S_{k(i)}}(\mathbf{x}_i) + r_i^{\text{CV}}\}\right]. \tag{A.3}$$

Appendix B: Simulation results for XBART-GP and its baselines

B.1 Simulation results on different functions

Figure 7 and Table 3 demonstrate the performance of XBART-GP versus other baseline methods. The results on the two functions, trig + poly and max, are consistent with the

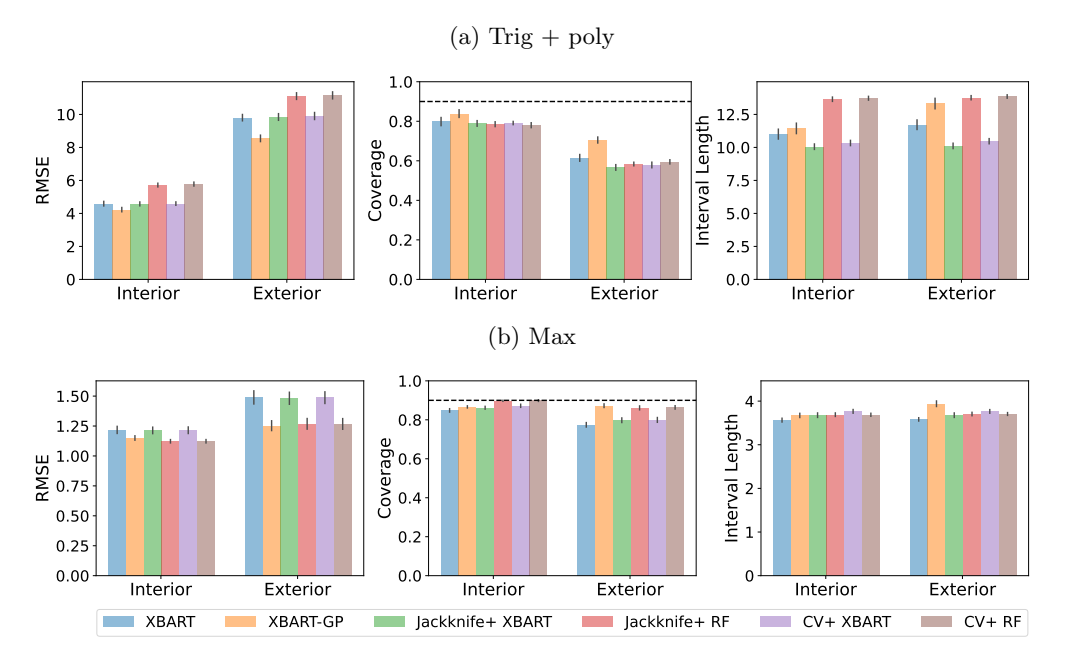


Figure 7: Visualization of simulation results in root mean square error (RMSE), interval coverage (Coverage), and interval length for interior and exterior points for tirg + poly and max functions. The horizontal dash line indicates the 90% target coverage level.

other two presented in the paper. It shows XBART-GP's ability to provide the most accurate prediction on both in-range and out-of-the-range data with almost desired coverage and slightly wider prediction intervals on various data generating processes.

B.2 Simulation results on increasing sample size

On interior points, XBART-based methods produce smaller RMSE than random forest methods. Among them, XBART-GP has the smallest RMSE overall. XBART and its Gaussian process extrapolation alternative have lower coverage than Jackknife methods when the sample size is minimal. But XBART-GP outperforms other methods on interior points as the sample size grows larger. XBART and XBART-GP produce the shortest intervals. The intervals of Jackknife+ XBART and CV+ XBART converge to XBART as the sample size increases.

N. (1 1	RMSE		Coverage		Interval length						
Method	Interior	Exterior	Interior	Exterior	Interior	Exterior					
Linear											
XBART-GP	1.756	2.506	0.881	0.816	5.709	6.717					
XBART	1.986	3.532	0.843	0.584	5.568	5.678					
Jackknife+ XBART	1.894	3.51	0.897	0.626	6.12	6.133					
Jackknife+ RF	2.975	4.598	0.834	0.656	8.499	8.55					
CV+XBART	1.883	3.466	0.9	0.651	6.366	6.384					
CV+RF	3.006	4.635	0.851	0.652	8.642	8.702					
Single index											
XBART-GP	4.582	10.631	0.871	0.474	13.938	15.854					
XBART	5.004	13.055	0.83	0.297	13.625	13.965					
Jackknife+ XBART	4.802	13.027	0.873	0.305	14.715	14.778					
Jackknife+ RF	8.077	17.068	0.765	0.263	19.592	19.689					
CV+XBART	4.754	13.097	0.897	0.327	15.725	15.78					
CV+RF	8.165	17.162	0.764	0.265	19.88	19.94					
		Trig +	poly								
XBART-GP	4.229	8.549	0.839	0.705	11.441	13.322					
XBART	4.591	9.805	0.798	0.615	11.007	11.718					
Jackknife+ XBART	4.577	9.845	0.789	0.567	10.054	10.115					
Jackknife+ RF	5.719	11.11	0.785	0.584	13.65	13.764					
CV+XBART	4.595	9.904	0.791	0.579	10.334	10.47					
CV+RF	5.778	11.156	0.78	0.595	13.726	13.857					
Max											
XBART-GP	1.15	1.253	0.866	0.873	3.672	3.94					
XBART	1.218	1.489	0.848	0.774	3.564	3.582					
Jackknife+ XBART	1.213	1.482	0.862	0.798	3.677	3.678					
Jackknife+ RF	1.123	1.268	0.898	0.861	3.689	3.704					
CV+XBART	1.215	1.487	0.872	0.8	3.765	3.764					
CV+ RF	1.123	1.267	0.899	0.864	3.687	3.705					

Table 3: Results of simulation comparing various approach on prediction interval. Columns are mean square error (RMSE), interval coverage (Coverage), and interval length (I.L.) on interior and exterior points for 4 different data generating processes. Time in seconds is presented in logarithm scale.

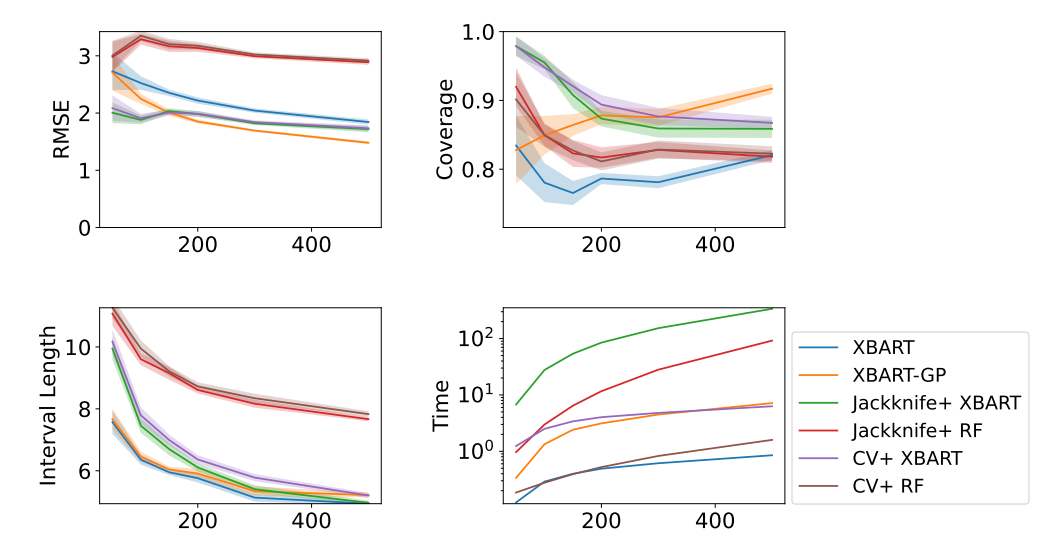


Figure 8: Results of simulation comparing various approach on prediction interval. Average RMSE, coverage, interval length on interior points, and running time at 90% level for all methods over 10 independent trials with increasing sample size from 50 to 500.